

## Abstract

The propagation of high-frequency elastic-flexural waves through an ice shelf was modeled by a full 3-D elastic models. These models based on the momentum equations that were written as the differential equations (model#1) and as the integro-differential equations (model#2). The integro-differential form implies the vertical integration of the momentum equations from the current coordinate  $z$  to the ice surface like, for instance, in the Blatter-Pattyn ice flow model (Pattyn, 2000, 2002). The sea water flow under the ice shelf is described by the wave equation (Holdsworth and Glynn, 1978). The numerical solutions were obtained by a finite-difference method. Numerical experiments were undertaken for a crevasse-ridden ice shelf (Freed-Brown et al., 2012) with different spatial periodicities of the crevasses. In this research the modeled positions of the band gaps in the dispersion spectra dependently on the spatial periodicities of the crevasses is investigated from the point of view of agreement of these positions with the Bragg's law. The investigation of the dispersion spectra shows that different models reveal different sensitivities of the dispersion spectra (in relation to the appearance of the band gaps in the spectra) dependently on the spatial periodicity of the crevasses and on the crevasses depth.

## Field equations

The two 3-D elastic models were considered in this work.

### Model#1. Basic equations.

The momentum equations are (e.g., Landau & Lifshitz, 1986; Lurie, 2005)

$$\begin{cases} \frac{\partial \sigma_{xx}}{\partial x} + \frac{\partial \sigma_{xy}}{\partial y} + \frac{\partial \sigma_{xz}}{\partial z} = \rho \frac{\partial^2 U}{\partial t^2}; \\ \frac{\partial \sigma_{yx}}{\partial x} + \frac{\partial \sigma_{yy}}{\partial y} + \frac{\partial \sigma_{yz}}{\partial z} = \rho \frac{\partial^2 V}{\partial t^2}; \\ \frac{\partial \sigma_{zx}}{\partial x} + \frac{\partial \sigma_{zy}}{\partial y} + \frac{\partial \sigma_{zz}}{\partial z} = \rho \frac{\partial^2 W}{\partial t^2}; \end{cases} \quad (1)$$

$$0 < x < L; y_1(x) < y < y_2(x); h_b(x, y) < z < h_s(x, y);$$

where  $\sigma_{ik}$  is the stress tensor,  $\rho$  is ice density;  $U, V, W$  are two horizontal displacements and vertical displacement, respectively. The geometry of the ice shelf is assumed to be given by lateral boundary functions  $y_{1,2}(x)$  at sides labeled 1 and 2 and functions for the surface and base elevations,  $h_{s,b}(x, y)$ , denoted by subscripts  $s$  and  $b$ , respectively.

The sub-ice water flow is described by the wave equation (Holdsworth and Glynn, 1978).

The wave equation is

$$\frac{\partial^2 W_b}{\partial t^2} = \frac{1}{\rho_w} \frac{\partial}{\partial x} \left( d_0 \frac{\partial P'}{\partial x} \right) + \frac{1}{\rho_w} \left( d_0 \frac{\partial P'}{\partial y} \right), \quad (2)$$

where  $\rho_w$  is sea water density;  $d_0(x, y)$  is the depth of the sub-ice water layer;  $W_b(x, y, t)$  is the vertical deflection of the ice-shelf base, and  $W_b(x, y, t) = W(x, y, h_b(x, y), t)$ ; and

$P'(x, y, t)$  is the deviation of the sub-ice water pressure from the hydrostatic value.

This model was considered, e.g., in (Konovalov, 2019, 2021).

### Model#2. Basic equations.

The momentum equations in the model#2 result of the integration of the momentum equations (1) in vertical direction like in the Blatter-Pattyn ice flow model (e.g. Pattyn, 2000, 2002)

The momentum equations are

$$\begin{cases} \frac{\partial}{\partial x} \int_z^{h_s} \sigma_{xx} dz + \frac{\partial}{\partial y} \int_z^{h_s} \sigma_{xy} dz - \sigma_{xz} = \rho \int_z^{h_s} \frac{\partial^2 U}{\partial t^2} dz; \\ \frac{\partial}{\partial x} \int_z^{h_s} \sigma_{yx} dz + \frac{\partial}{\partial y} \int_z^{h_s} \sigma_{yy} dz - \sigma_{yz} = \rho \int_z^{h_s} \frac{\partial^2 V}{\partial t^2} dz; \\ \frac{\partial}{\partial x} \int_z^{h_s} \sigma_{xz} dz + \frac{\partial}{\partial y} \int_z^{h_s} \sigma_{zy} dz - \sigma_{zz} = \rho g(h_s - z) + \rho \int_z^{h_s} \frac{\partial^2 W}{\partial t^2} dz; \end{cases} \quad (3)$$

$$0 < x < L; y_1(x) < y < y_2(x); h_b(x, y) < z < h_s(x, y);$$

The sub-ice water flow is described by the wave equation (2).

## Results

### The ice-shelf geometry

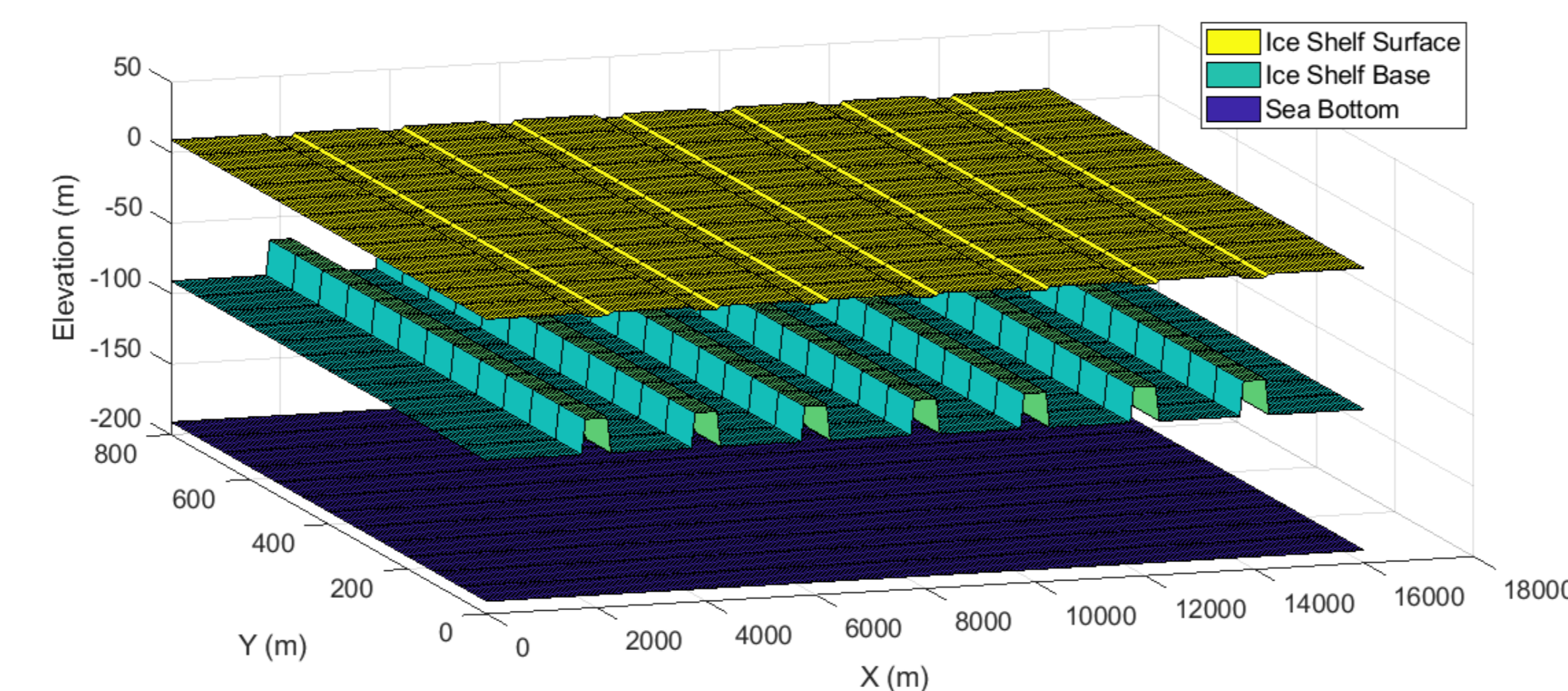


Fig.1. The crevasse-ridden ice-shelf geometry and the cavity geometry that were considered in the numerical experiments. Spatial periodicity of the crevasses is equal to 2.0 km.

### The dispersion spectra

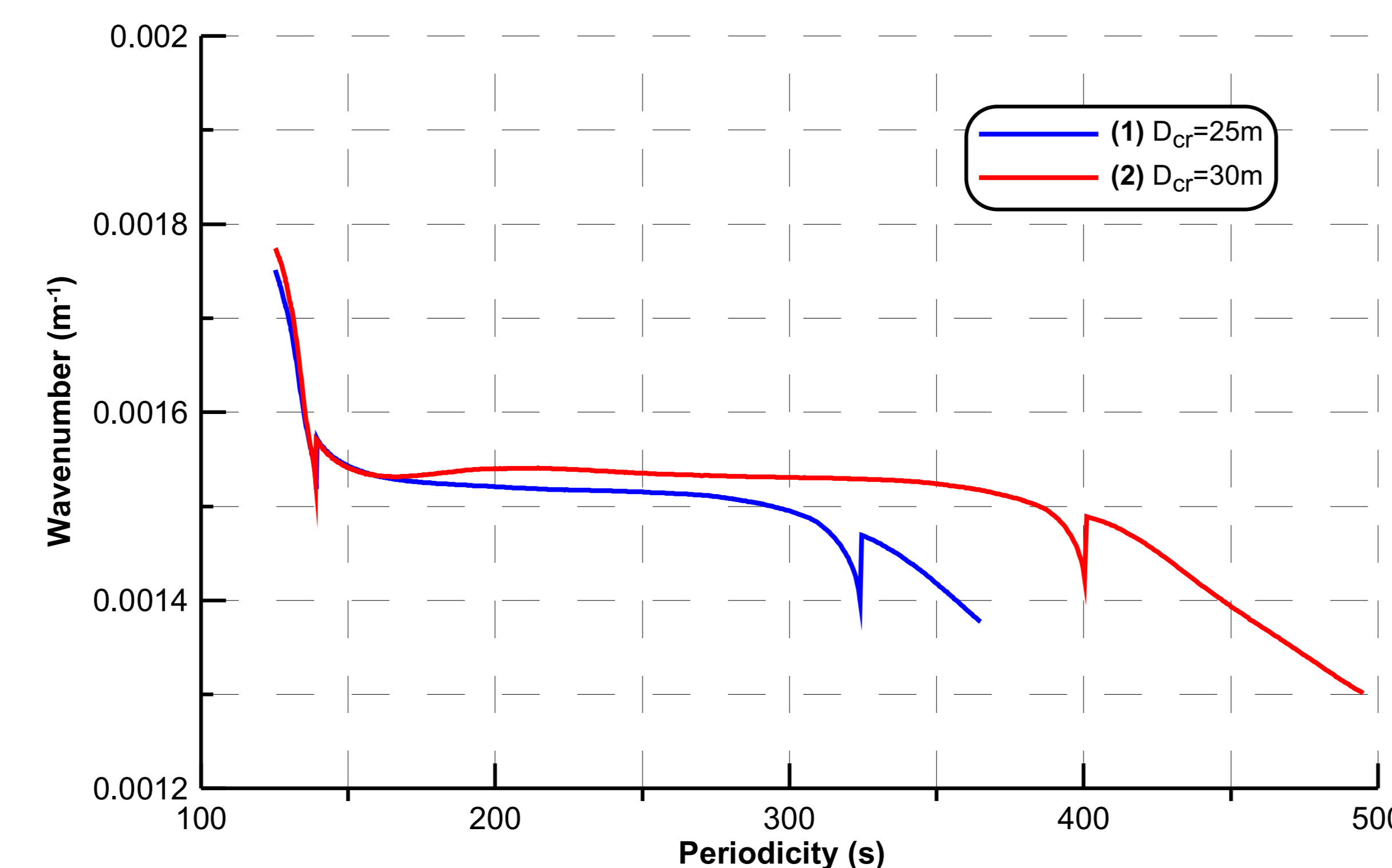


Fig.2. The dispersion spectrum obtained for the crevasse-ridden ice shelf by the model#1. 1 –  $D_{cr}=25m$ ; 2 -  $D_{cr}=30m$ . ( $D_{cr}$  is the crevasses depth). Spatial periodicity of the crevasses is equal to 2 km. Young's modulus  $E = 9 GPa$ , Poisson's ratio  $\nu = 0.33$ .

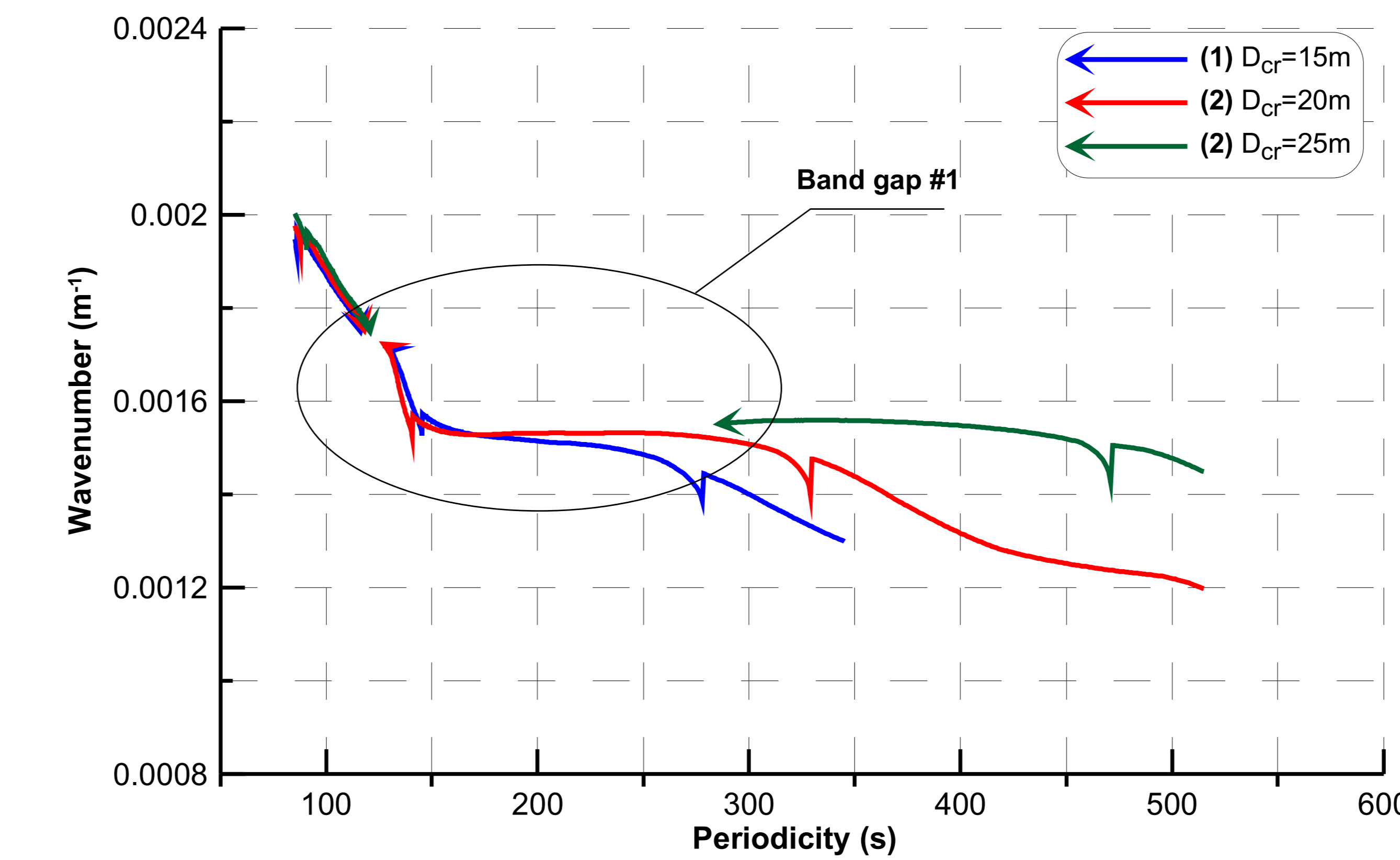


Fig.3. The dispersion spectrum obtained for the crevasse-ridden ice shelf by the model#2. 1 –  $D_{cr}=15m$ ; 2 –  $D_{cr}=20m$ ; 3 –  $D_{cr}=25m$  ( $D_{cr}$  is the crevasses depth). Spatial periodicity of the crevasses is equal to 2 km. Young's modulus  $E = 9 GPa$ , Poisson's ratio  $\nu = 0.33$ .

### The band gap location in the dispersion spectra

Table#1. The first band gap location in the dispersion spectra obtained by the model#1 for different spatial periodicities of the crevasses ( $T_{cr}$ ) and for different values of the crevasses depth ( $D_{cr}$ )

$T_{cr}(km)$ $D_{cr}(m)$	20 m	25 m	30 m	35 m	40 m	The first wavenumber derived from the Bragg's law ( $km^{-1}$ )
1.8 km		doesn't appear	doesn't appear	1.723..1.755 $km^{-1}$	1.722..1.771 $km^{-1}$	1.745
2.0 km		doesn't appear	doesn't appear	1.537..1.565 $km^{-1}$		1.57
2.2 km	doesn't appear	doesn't appear	1.394..1.422 $km^{-1}$	1.41..1.438 $km^{-1}$		1.43

Table#2. The first band gap location in the dispersion spectra obtained by the model#2 for different spatial periodicities of the crevasses ( $T_{cr}$ ) and for different values of the crevasses depth ( $D_{cr}$ )

$T_{cr}(km)$ $D_{cr}(m)$	15 m	20 m	25 m	30 m	The first wavenumber derived from the Bragg's law ( $km^{-1}$ )
1.8 km	1.687..1.715 $km^{-1}$	1.7..1.8 $km^{-1}$			1.745
2.0 km	1.715..1.745 $km^{-1}$	1.723..1.746 $km^{-1}$	1.552..1.742 $km^{-1}$		1.57
2.2 km		doesn't appear	1.728 .. - $km^{-1}$		1.43

## Summary

The performed numerical experiments reveal that the model#2 is more sensitive than the model#1 in the context of the considered ice shelf response to the ocean wave impact. The distinction is in the threshold value of the depth of the crevasses penetration to the ice shelf, at which the band gaps that should appear accordingly the Bragg's law, in fact, arise in the dispersion spectra obtained by the models. Essentially the model#2 based on the depth-integrated momentum equations provides the smaller threshold value, which depends on the spatial periodicity of the crevasses.

## References

- Holdsworth, G., & Glynn, J.: Iceberg calving from floating glaciers by a vibrating mechanism. *Nature*, 274, 464-466, 1978
- Freed-Brown, J., Amundson, J., MacAyeal, D., & Zhang, W. Blocking a wave: Frequency band gaps in ice shelves with periodic crevasses. *Annals of Glaciology*, 53(60), 85-89. doi:10.3189/2012AoG60A120, 2012.
- Landau, L.D., Lifshitz, E.M.: *Theory of Elasticity* (3rd ed.). Oxford: Butterworth-Heinemann, (Vol. 7), 1986
- Lurie, A.I.: *Theory of Elasticity*. Berlin: Springer, (Foundations of Engineering Mechanics), 2005
- Konovalov, Y.V.: Ice-shelf vibrations modeled by a full 3-D elastic model. *Annals of Glaciology*, 60(79) 68-74, doi: 10.1017/aog.2019.9, 2019.
- Konovalov, Y.V.: Abatement of Ocean-Wave Impact by Crevasses in an Ice Shelf. *J. Mar. Sci. Eng. 9*, 46. doi: 10.3390/jmse9010046, 2021.
- Pattyn F.: Ice-sheet modeling at different spatial resolutions: focus on the grounding zone, *Annals of Glaciology*, 31, 211-216, 2000.
- Pattyn F.: Transient glacier response with a higher-order numerical ice-flow model, *Journal of Glaciology*, 48, 467-477, 2002.